Pseudohalogens for Dye-Sensitized TiO 2 Photoelectrochemical Cells

ARTICLE *in* THE JOURNAL OF PHYSICAL CHEMISTRY B · JULY 2001

Impact Factor: 3.3 · DOI: 10.1021/jp004411d

4 AUTHORS, INCLUDING:

Peter Searson
Johns Hopkins University
297 PUBLICATIONS **11,668** CITATIONS

SEE PROFILE

Pseudohalogens for Dye-Sensitized TiO_2 Photoelectrochemical Cells

Gerko Oskam,*,† Bryan V. Bergeron,‡ Gerald J. Meyer,‡,† and Peter C. Searson*,†

Department of Materials Science and Engineering, and Department of Chemistry, The Johns Hopkins University, Baltimore, Maryland 21218

Received: December 7, 2000; In Final Form: April 16, 2001

In this paper, we report on the preparation and characterization of two pseudohalogen redox couples for dye-sensitized TiO_2 photoelectrochemical cells. The equilibrium potentials of the $(SeCN)_2/SeCN^-$ and $(SCN)_2/SCN^-$ couples are respectively 0.19 and 0.43 V more positive than for the I_3^-/I^- couple, providing the opportunity to determine the influence of the redox potential on the open circuit photovoltage. With the sensitizer *cis*-$Ru(dcb)_2(NCS)_2$ (N3), the incident photon-to-current conversion efficiency was 20% for the $(SeCN)_2/SeCN^-$ couple and 4% for the $(SCN)_2/SCN^-$ couple. Transient absorbance measurements showed that the quantum yield for electron injection is independent of the pseudohalogen redox couple and that the regeneration rates of the dye decrease in the order $I^- > SeCN^- > SCN^-$. The effects of the redox potential on open circuit photovoltage were determined by independent measurement of the dependence of the sensitized TiO_2 working electrode and the platinum counter electrode potentials on the cell voltage.

Introduction

Since the first report of high energy conversion efficiencies for dye-sensitized TiO_2 solar cells in 1991,[1] there has been intense interest in understanding the parameters that control cell operation and performance.[2] Energy conversion efficiencies of about 10% (air-mass 1.5 solar irradiation) have been reported for regenerative photoelectrochemical cells based on nanocrystalline TiO_2 films sensitized with *cis*-$Ru(dcb)_2(NCS)_2$ (known as N3, where dcb is 4,4′-$(CO_2H)_2$-2,2′-bipyridine) using tri-iodide/iodide in an organic solvent.[3] Current research is focused on the development of new dyes with absorbance profiles that better match the solar spectrum and methods to increase the operational voltage either through increases in the open circuit voltage (V_{oc}) or the fill factor.[2] The redox couple is expected to play an important role in determining cell performance; however, its influence is not well understood.

Figure 1 shows a simplified band diagram illustrating possible effects of the redox couple on the cell energetics. The open circuit potential is determined by the difference between the Fermi energies of the illuminated transparent conducting oxide (TCO) with the nanocrystalline TiO_2 film and the platinum-coated TCO electrode. If it is assumed that the Fermi energy of the TCO/dye-sensitized TiO_2 electrode is independent of the redox couple and that the Fermi energy of the TCO/platinum counter electrode is close to the redox energy, a considerable increase in V_{oc} could be achieved if the tri-iodide/iodide electrolyte were replaced by the thiocyanate/thiocyanogen couple. However, the dependence of V_{oc} on the redox energy may be influenced by a number of factors. For example, the Fermi energy of the TCO electrode with the dye-sensitized TiO_2 film may shift with redox energy. In addition, the kinetics of electron transport and charge-transfer processes have been shown to be important factors in determining the cell performance. Under open circuit conditions, the rate of electron injection is equal to the rate of the loss processes such as transfer of electrons from the TiO_2 either back to the oxidized dye molecules or to the oxidized redox species in solution (e.g., I_3^-).[2−4] Very low light-to-electrical energy conversion efficiencies reported for one-electron, outer-sphere redox couples have been attributed to the fast kinetics and efficient recombination of the injected electron with the oxidized species.[5,6] The redox couple is also expected to influence other processes such as reduction of the oxidized[7] or excited dye molecules,[8] the reduction of the oxidized form(s) of the redox couple at TiO_2,[3−5] the electron-transfer kinetics at the counter electrode,[9] adsorption

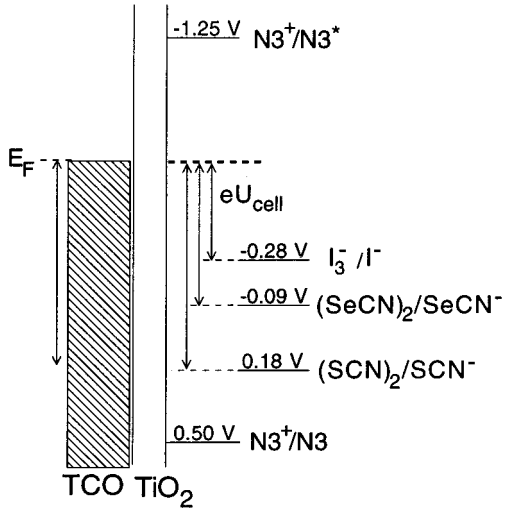

Figure 1. Schematic energy diagram for a transparent conductive electrode (TCO) contact to a TiO_2 nanostructured film sensitized with the N3 dye, where N3 is *cis*-$Ru(dcb)_2(NCS)_2$, with the indicated redox couples. The reduction potentials for the N3 ground and excited states were taken from ref 3, and the three redox couples were measured in this work. The potentials are reported with respect to the Ag^+/Ag reference in acetonitrile. The arrows indicating the cell voltage, U_{cell}, illustrate the maximum possible voltages for the respective redox couples. The arrows on the left indicate that the TCO Fermi energy, E_F, may also shift upon changing the redox couple.

* Corresponding authors. E-mail: oskam@jhu.edu. E-mail: searson@jhu.edu. Fax: (410) 516−5293.

† Department of Materials Science and Engineering.

‡ Department of Chemistry.

10.1021/jp004411d CCC: $20.00
Published on Web 06/28/2001

on the electrode surface,[10,11] ion-pairing with the dye,[12] and charge transport in the semiconductor film and in solution.[13]

In this paper, we report on the preparation and characterization of two pseudohalogen redox couples, $(SCN)_2/SCN^-$ and $(SeCN)_2/SeCN^-$, with more positive equilibrium potentials than the commonly utilized I_3^-/I^-. These redox couples were used in regenerative solar cells based on N3-sensitized nanocrystalline TiO_2, and their influence on the cell performance was determined using optical and photoelectrochemical measurements.

Experimental Methods

Materials. The *cis*-$Ru(dcb)_2(NCS)_2$ dye, N3, was synthesized following a method reported previously (see also the Supporting Information).[14] Reagents were obtained and used as follows: $Pb(SCN)_2$ (Aldrich, 99.5%); CH_3CN (HPLC grade); Br_2 (Aldrich, 99.5+%); NaSCN (Alfa-Aesar, 98%); KSeCN (Alfa-Aesar, 98.5%); NaI (Aldrich, 99+%); and $LiClO_4$ (99.99%). HPLC grade acetonitrile was used as received.

Electrolyte Solutions. The electrolyte solutions used for the experiments consisted of 25 mM of the oxidized form of the redox couple, 100 mM of the reduced form, and 0.25 M $LiClO_4$ in acetonitrile.

The 25 mM $(SCN)_2$ + 100 mM NaSCN solution was prepared as follows: 2.5 mmol $Pb(SCN)_2$ was added to 50 mL acetonitrile, and the suspension was cooled to 0 °C using an ice bath. With stirring, 2.5 mmol Br_2 in 25 mL acetonitrile was added slowly such that the suspension was allowed to turn colorless before adding more. The resulting suspension was filtered to remove $PbBr_2$, resulting in a clear, colorless solution of thiocyanogen, $(SCN)_2$. Absorbance spectra of the solution showed a peak at 295 nm characteristic of $(SCN)_2$, and using an extinction coefficient of 140 M^{-1} cm^{-1}, the thiocyanogen concentration corresponded to 100% reaction efficiency.[15] Subsequently, 10 mmol NaSCN in 25 mL acetonitrile was added dropwise, resulting in a light yellow solution. Solutions with more than 50 mM $(SCN)_2$ and more than 100 mM NaSCN were unstable, resulting in precipitation of parathiocyanogen, $(SCN)_x$.[16] The $(SeCN)_2/SeCN^-$ solutions were prepared in a similar manner. A solution of 5 mmol KSeCN in 50 mL acetonitrile was reacted with 2.5 mmol Br_2 in 25 mL acetonitrile with stirring, under ice, and in the dark. The resulting suspension was filtered to remove precipitated KBr, resulting in a yellow selenocyanogen solution, which darkened in color upon slowly adding 10 mmol KSeCN in 25 mL acetonitrile. The 25 mM I_3^- + 100 mM I^- solution was prepared by adding 12.5 mmol NaI and 2.5 mmol I_2 to 100 mL acetonitrile.

$LiClO_4$ was added to all solutions to a concentration of 0.25 M in order to increase the conductivity and to obtain the same Li^+ concentration in the three systems. For the $(SeCN)_2/SeCN^-$ solutions, $KClO_4$ precipitated upon adding $LiClO_4$, resulting in a slightly lower ionic strength. Solutions were prepared prior to each set of experiments.

Electrochemistry. Electrochemical characterization of the redox couples was performed in a three-electrode cell using a platinum rotating disk electrode with an area of 0.031 cm^2. The counter electrode was separated from the working electrode by a coarse glass frit. The reference electrode consisted of a Ag wire in 0.1 M $AgClO_4$ + 0.25 M $TBABF_4$ in acetonitrile, separated from the working electrode compartment with a porous Vycor tip. The reference electrode was positioned close to the working electrode using a Luggin capillary. The potential of the reference electrode was determined by recording cyclic voltammograms at a platinum wire in 0.01 M ferrocene + 0.25 M $TBABF_4$ in acetonitrile. The reference potential was 0.04 V with respect to the ferrocene/ferrocenium redox couple, in good agreement with previously reported values, and approximately 0.35 V versus aqueous SCE.[17]

TiO_2 Preparation. Nanocrystalline anatase TiO_2 was prepared using a solution phase method.[18] Titanium tetraisopropoxide ($Ti-(O-^iPr)_4$) was used as a precursor, and the colloid was prepared in aqueous solution acidified with HNO_3 to pH 1. A typical procedure was as follows: 15 mL $Ti-(O-^iPr)_4$ was added dropwise to 185 mL water acidified with 1.3 mL concentrated HNO_3 under vigorous stirring at room temperature. The colloidal solution was then peptized at 85 °C with stirring in an open flask for about 12 h in order to remove volatile reaction products (viz. 2-propanol). The colloid was aged at 200 °C in a sealed titanium pressure vessel for 16 h, resulting in a white colloid with a TiO_2 concentration of about 80 g/L. The colloid was then condensed to 160 g/L under low heat (T < 60 °C). The TiO_2 paste was mixed with 40 wt % poly(ethylene glycol) (PEG, M_W = 20 000) with stirring for 14 h at room temperature. Films were prepared on 16 Ω cm TCO (In_2O_3:Sn) on glass (Libby Owens Ford) using an adhesive tape mask and a glass rod, and after 20 min of air-drying, the films were heated at 450 °C for 30 min. The optical transmission of the TCO films on glass was about 80% in the wavelength range from 350 to 800 nm. The thickness of the TiO_2 films determined using profilometry was about 4 μm, and the optical density of the films was smaller than 0.2 at wavelengths larger than 450 nm. No surface treatments were used to increase the open circuit potential. The films were sensitized by immersion in *cis*-$Ru(dcb)_2(SCN)_2$, (N3), in ethanol for 24 h. The absorbance of the dye sensitized films was about 1.2 at 520 nm.

Photoelectrochemistry. Incident photon-to-current conversion efficiency (IPCE) measurements were performed in a three-electrode cell with the dye-sensitized TiO_2/TCO electrode as working electrode and a platinum coated TCO glass counter electrode under short circuit conditions. The spacing between the two electrodes was 0.635 cm, and the exposed cell area was 0.3 cm^2. Fresh samples were used for each redox couple. The reference electrode consisted of a Ag wire in 0.1 M $AgClO_4$ and 0.25 M $TBABF_4$ in acetonitrile, positioned in a separate compartment and connected to the cell by means of a small Teflon tube filled with the same solution as in the cell. The cell was illuminated from the TiO_2 side of the cell using an arc lamp and monochromator fitted with a fiber optic cable and collimating lens.

Absorbance. Steady-state absorption measurements were performed on a Hewlett-Packard 8453 diode array spectrophotometer with a TiO_2 film on a microscope slide in 0.25 M $LiClO_4$ in acetonitrile solution as a reference.

Transient spectra were acquired as previously described.[19] A pulse of approximately 7 ns at 532 nm (14 mJ/pulse) from a Surelite II Nd:YAG Q-switched laser was used as the excitation source. A white light source was the probe beam (150 W Xe, Applied Photophysics, operating in pulsed mode) and was positioned normal to the excitation beam and was focused on the exposed TiO_2 surface. The excitation/probe orientation was chosen to minimize scattered light reaching the detector. The sample was protected from UV and IR light using glass and water filters positioned between the lamp and the sample; scattered laser light was attenuated using glass filters between the sample and monochromator. The transmitted light was collected and refocused on the entrance slit of a monochromator (Applied Photophysics) and detected using a photomultiplier (Hamamatsu R928). The data were digitized and stored on a digital oscilloscope (LeCroy 9450). The data shown were

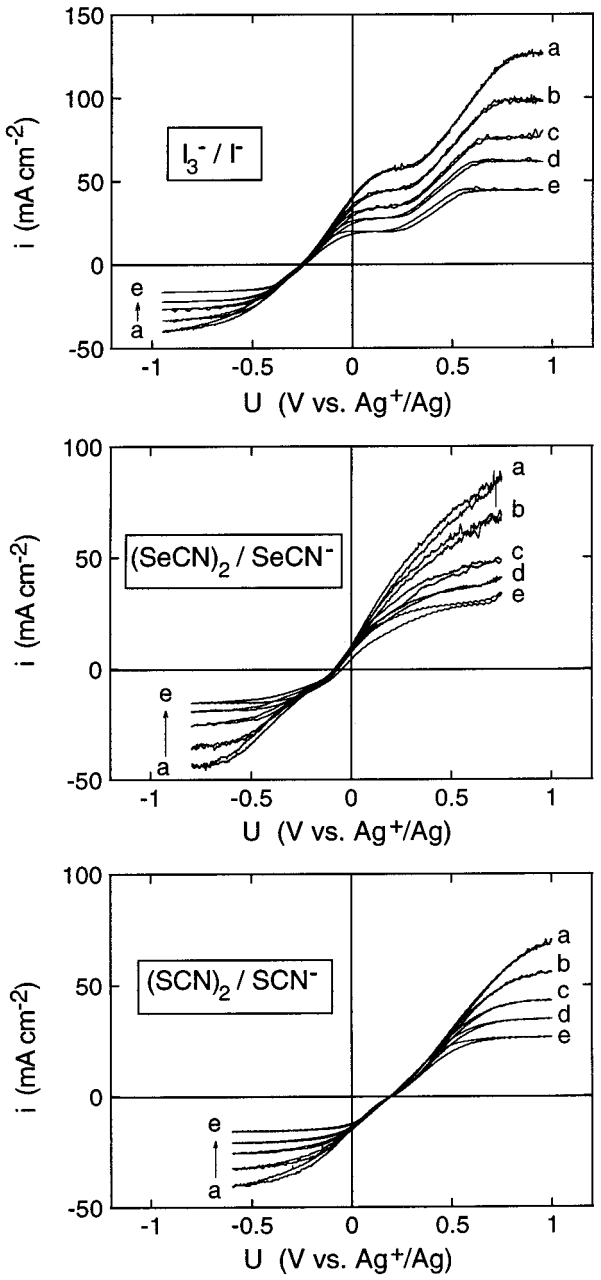

Figure 2. Rotating disk cyclic voltammograms in 0.25 M $LiClO_4$ in acetonitrile solutions with the I_3^-/I^-, $(SeCN)_2/SeCN^-$, and $(SCN)_2/SCN^-$ redox couples as a function of rotation rate. All solutions contain 25 mM of the oxidized (i.e., I_3^-) and 100 mM of the reduced (i.e., I^-) species. The rotation rates were (a) 800 rpm, (b) 500 rpm, (c) 300 rpm, (d) 200 rpm, and (e) 100 rpm, respectively. The scan rate was 50 mV s^{-1}.

acquired by averaging 40−200 laser pulses (typically 80) at a repetition rate of 1 Hz.

Results and Discussion

Figure 2 shows the current−potential curves for the I_3^-/I^-, $(SeCN)_2/SeCN^-$, and $(SCN)_2/SCN^-$ redox couples on a platinum rotating disk electrode (RDE) in 0.25 M $LiClO_4$ in acetonitrile as a function of the rotation rate. In all cases, the maximum reduction and oxidation plateau current densities were proportional to the square-root of the rotation rate in accordance with the Levich equation.[20] These results indicate that the charge transfer reactions are diffusion limited at sufficiently large overpotentials. The I_3^-/I^- couple is characterized by two oxidation waves: the wave at 0.1 V corresponds to the oxidation

TABLE 1: Redox Reactions and Corresponding Diffusion Coefficients and Equilibrium Redox Potentials for the Pseudohalogen Redox Couples[a]

	D (cm^2 s^{-1})	redox reaction	U^0 (vs RE)[b]
I_3^-	1.6×10^{-5}	$I_3^- + 2e^- \leftrightarrow 3I^-$	−0.28
I^-	1.7×10^{-5}		
$(SeCN)_2$	1.4×10^{-5}	$(SeCN)_2 + 2e^- \leftrightarrow 2SeCN^-$	−0.09
$SeCN^-$	1.6×10^{-5}		
$(SCN)_2$	1.5×10^{-5}	$(SCN)_2 + 2e^- \leftrightarrow 2SCN^-$	0.18
SCN^-	1.2×10^{-5}		

[a] The redox potentials are calculated from the Nernst equation for unit concentrations (assuming unit activity constants). [b] RE = Ag in 0.1 M $AgClO_4$ + 0.25 M $TBABF_4$ in acetonitrile: U ≈ 0.35 V vs SCE

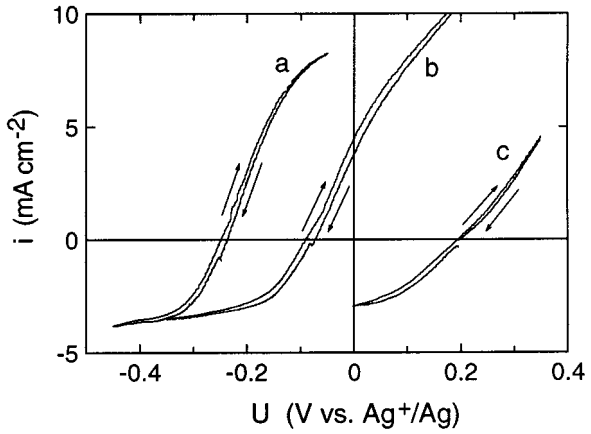

Figure 3. Cyclic voltammograms in 0.25 M $LiClO_4$ in acetonitrile solutions with the (a) I_3^-/I^-, (b) $(SeCN)_2/SeCN^-$, and (c) $(SCN)_2/SCN^-$ redox couples at 25 mM/100 mM concentrations at a slow scan rate of 0.5 mV s^{-1}. The average potential where the current is zero corresponds to the redox potential of the couple.

of I^- to I_3^-, whereas the second wave at 0.8 V has been ascribed to the oxidation of I_3^- to I_2.[21] For the $(SCN)_2/SCN^-$ couple there is no indication of $(SCN)_3^-$ formation, in agreement with previous reports.[22,23] Electropolymerization to $(SCN)_x$ was observed at higher concentrations and temperatures and is a limitation for the practical use of the $(SCN)_2/SCN^-$ couple.[16] The electrochemistry of the $(SeCN)_2/SeCN^-$ couple is similar to that of the $(SCN)_2/SCN^-$ couple; however, electropolymerization was not observed. The redox reactions for the three couples in these solutions and the diffusion coefficients of the electroactive species, determined from the rotation rate dependence of the diffusion-limited currents, are presented in Table 1. The diffusion coefficients for the three redox couples are close to 1.4×10^{-5} cm^2 s^{-1}, and are in good agreement with values reported in the literature.[20,22,23]

Figure 3 shows current−potential curves measured at 0.5 mV s^{-1} for the three redox couples in the potential range close to the equilibrium potential. It can be seen that the rate of increase of the current with potential for the triiodide/iodide and the selenocyanogen/selenocyanate couples are very similar, whereas the kinetics for the thiocyanogen/thiocyanate couple are clearly slower. The open circuit potentials correspond to the equilibrium potentials for the reactions, and the corresponding standard equilibrium potentials (at unit concentrations) are shown in Table 1. The standard equilibrium potential for the I_3^-/I^- couple (about 0.07 V(SCE)) is significantly more negative than in aqueous solution where the standard equilibrium potential is 0.25 V(SCE).[25] The standard equilibrium potential of the $(SeCN)_2/SeCN^-$ couple of 0.26 V(SCE) is in good agreement with a previous report for this redox couple in acetonitrile;[24] $(SeCN)_2$ is not stable in aqueous solution. For the $(SCN)_2/SCN^-$ couple,

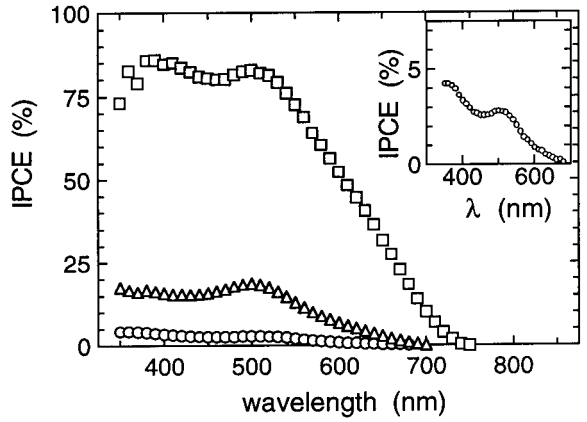

Figure 4. Incident photon-to-current conversion efficiencies versus wavelength for dye-sensitized TiO_2 photoelectrochemical cells with 0.25 M $LiClO_4$ in acetonitrile solutions with the (□) I_3^-/I^-, (△) $(SeCN)_2/SeCN^-$, and (○) $(SCN)_2/SCN^-$ redox couples at 25 mM/100 mM concentrations. The inset shows the IPCE curve for the $(SCN)_2/SCN^-$ redox couple on a smaller scale.

the standard equilibrium potential in both acetonitrile and in aqueous solution is 0.53 V(SCE).[25]

Figure 4 shows the incident photon-to-current conversion efficiency (IPCE) for cells with the three redox couples in 0.25 M $LiClO_4$ in acetonitrile. The IPCE for the cell with the I_3^-/I^- couple is about 80% between 400 and 520 nm, which corresponds to an absorbed photon-to-current conversion efficiency of about 100%, taking into account the 80% transmission of the TCO-coated glass substrate. The cells with the $(SeCN)_2/SeCN^-$ couple have an IPCE of about 20%, whereas the cells with $(SCN)_2/SCN^-$ couple show an IPCE of about 4%. To our knowledge, these pseudohalogen redox couples are the first alternatives to the I_3^-/I^- couple that show significant conversion efficiency for the N3 dye. The equilibrium potentials for these redox couples span about 0.45 V, suggesting that a wide range of possible pseudohalogen redox couples can be used in the dye-sensitized TiO_2 solar cells.

Transient absorbance measurements were performed on TiO_2 films sensitized with the N3 dye in 0.25 M $LiClO_4$ in acetonitrile with and without NaI, NaSCN, or KSeCN. The kinetics of dye regeneration by recombination of the injected electrons in TiO_2 with the oxidized dye or reduction by the reducing agent in solution can be directly probed.[7] The wavelength (500 nm) was chosen to monitor the recovery of the dye since the oxidized forms of the reducing agents do not absorb light appreciably at this wavelength. We note that a small absorption for I_2^- is seen at this wavelength; however, this does not significantly affect the results.[26]

Figure 5 shows the absorbance change after a 532 nm laser pulse for dye-sensitized TiO_2 films in 0.25 M $LiClO_4$ in acetonitrile versus time at 500 nm. The laser pulse generates the excited state of the dye, which then injects an electron into the TiO_2 within the 10 ns instrument response time. Hence, oxidized dye molecules are formed immediately after the laser pulse, resulting in a decrease of the absorbance at 500 nm. The magnitude of the initial absorption change is directly proportional to the quantum yield for electron injection. In the absence of an electron donor, all the injected electrons recombine with oxidized dye. Complete recombination requires milliseconds and is not shown.

Also shown in Figure 5 are the absorbance changes in the presence of 0.1 M I^-, $SeCN^-$, or SCN^- in acetonitrile with 0.25 M $LiClO_4$. The initial absorption change is the same as in the absence of the electron donor in solution, within experimental error, indicating that the injection yield is the same in the presence of these redox active electrolytes. Following electron transfer into TiO_2, the dye can be regenerated by the electron in TiO_2 or competitively by the external electron donor. In the presence of iodide, the dye molecule is rapidly regenerated within 500 ns, thereby inhibiting significant recombination from electrons in the TiO_2. In the presence of selenocyanate, only a small fraction of the oxidized dye remains 4.5 μs after the laser pulse, indicating that the selenocyanate anion is also capable of regenerating the dye, although the regeneration rate is much slower than in the iodide solution. In the thiocyanate solution, the regeneration of the dye is very slow, and can barely be distinguished from the transient absorbance spectrum without thiocyanate.

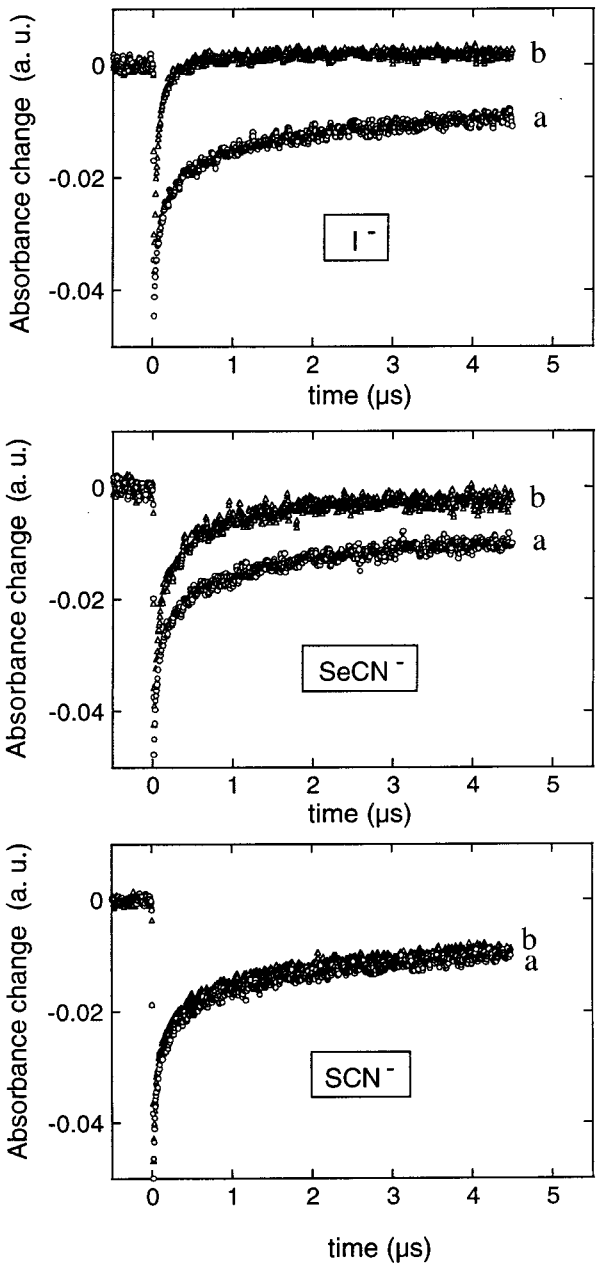

Figure 5. Transient absorbance measurements for dye-sensitized TiO_2 films in 0.25 M $LiClO_4$ in acetonitrile solutions with 100 mM NaI, 100 mM KSeCN, and 100 mM NaSCN, respectively. The change in the absorbance at 500 nm is plotted versus time after the laser pulse. Curve "a" corresponds to 0.25 M $LiClO_4$ in acetonitrile only, and curve "b" represents the same sample after adding the electron donor to the solution.

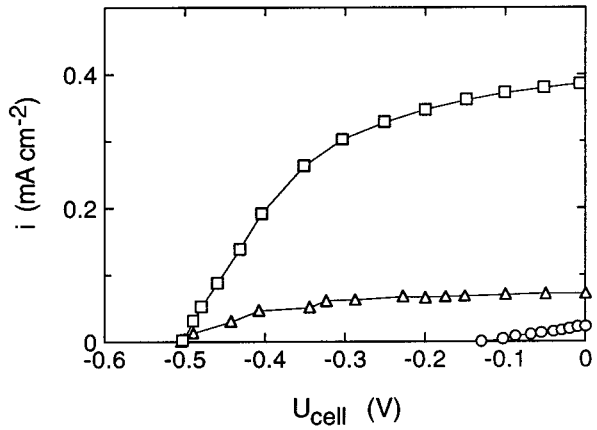

Figure 6. Photocurrent versus voltage curves for dye-sensitized TiO_2 photoelectrochemical cells with 0.25 M $LiClO_4$ in acetonitrile solutions with the (□) I_3^-/I^-, (△) $(SeCN)_2/SeCN^-$, and (○) $(SCN)_2/SCN^-$ redox couples at 25 mM/100 mM concentrations. Monochromatic green light (500 nm) was used and the light intensity was 1.3 mWcm^{-2} in all cases.

These results show that electron transfer from the TiO_2 back to the oxidized dye may play a significant role in dye regeneration in the presence of the $(SeCN)_2/SeCN^-$ couple, and a dominant role for the $(SCN)_2/SCN^-$ couple. Note that the electron injection yield is independent of the electron donors and their counterions due to the 0.25 M concentration of Li^+.[27] The results indicate that the decrease in IPCE with more positive redox potential can be attributed to slower kinetics for the regeneration of the dye.

Figure 6 shows current−voltage curves for cells with the three redox couples at the same monochromatic (500 nm) light intensity. The short-circuit current is highest for the I_3^-/I^- couple and lowest for the $(SCN)_2/SCN^-$ couple, in agreement with the IPCE results. In addition, the open circuit voltage significantly increases from 0.15 V for the $(SCN)_2/SCN^-$ to 0.55 V for the $(SeCN)_2/SeCN^-$ and I_3^-/I^- couples. A surprising result is the observation that the open circuit voltage for the $(SeCN)_2/SeCN^-$ and I_3^-/I^- couples are almost the same while the IPCE and the short-circuit current are a factor of four lower for the $(SeCN)_2/SeCN^-$ couple.

To determine the energetics of cells with the three redox couples, the potentials of the TCO/dye-sensitized TiO_2 working electrode (U_{TCO,TiO_2}) and the TCO/Pt counter electrode ($U_{TCO,Pt}$) were measured simultaneously with respect to a reference electrode during the current−voltage measurements. Figure 7 shows the potentials of the two electrodes versus the cell voltage for the cells with the different redox couples under the same illumination conditions as in Figure 6.

From Figure 7 it can be seen that under short circuit conditions, the potentials of the working and counter electrodes are the same. In all cases, $U_{TCO,Pt}$ is shifted to slightly more negative potentials than the equilibrium potential of the redox couple due to the overpotential needed to reduce the oxidized form of the redox couple. At intermediate cell voltages, $U_{TCO,Pt}$ shows a weak logarithmic dependence on the cell voltage as the current at the TCO/Pt electrode is exponentially dependent on the overpotential. $U_{TCO,Pt}$ reaches the equilibrium potential of the redox couple at V_{oc} where the current is zero: −0.24 V for I_3^-/I^-, −0.08 V for $(SeCN)_2/SeCN^-$, and 0.19 V for $(SCN)_2/SCN^-$. U_{TCO,TiO_2} varies linearly with the cell voltage in the plateau current regime, whereas it saturates upon approaching the open circuit voltage. With the Fermi energy of the Pt-coated TCO electrode pinned at the energy of the redox couple, the Fermi energy of TCO/dye-sensitized TiO_2 electrode is shifted

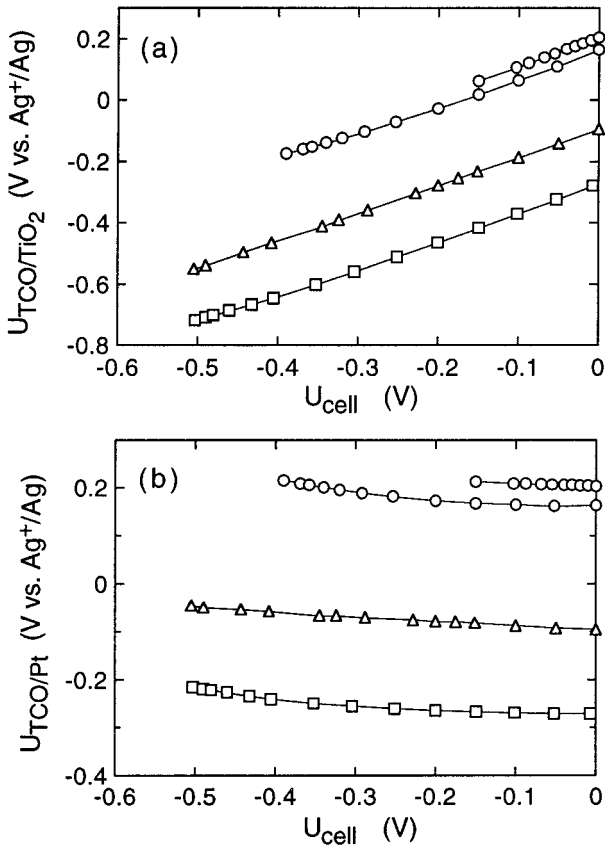

Figure 7. The potentials of the (a) working electrode (U_{TCO,TiO_2}) and (b) counter electrode ($U_{TCO,Pt}$) versus the cell potential recorded concurrently with the current−voltage curves shown in Figure 6 for the (□) I_3^-/I^-, (△) $(SeCN)_2/SeCN^-$, and (○) $(SCN)_2/SCN^-$ redox couples at 25 mM/100 mM concentrations. For the $(SCN)_2/SCN^-$ solution, a second curve is shown for clarity at a white light intensity of 95 mWcm^{-2} where the open circuit potential is 0.40 V and the short-circuit current is 0.22 mA cm^{-2}. It can be concluded that the there is only a small shift in the curves over a factor 73 change in light intensity.

to more negative potentials due to the build up of electrons injected by the dye under illumination. As a result, it is observed that U_{TCO,TiO_2} under open circuit conditions is different for the three redox couples. We note that even though the open circuit voltages for the I_3^-/I^- and the $(SeCN)_2/SeCN^-$ solutions are the same, $U_{TCO,Pt}$ and U_{TCO,TiO_2} are 0.16 V more positive in the $(SeCN)_2/SeCN^-$ solution. This is important since it is the absolute potentials and not the cell voltages that determine the stability of the solvent and electrolyte.

Figure 8 shows energy diagrams of the cells for the three redox couples constructed from the results shown in Figure 7. We assume that the energy levels of the dye do not depend on the redox couple. It can be seen that under both open circuit and short-circuit conditions, the potential of the TCO/dye-sensitized TiO_2 electrode is shifted with the redox potential. In addition, the diagrams under short-circuit conditions show that the driving force for the regeneration of the dye and the conversion efficiency decrease with increasing redox potential from I_3^-/I^- to $(SCN)_2/SCN^-$. We therefore conclude that the decrease in IPCE associated with more positive redox potentials is due to the decrease in driving force and, hence, the slower rate of dye regeneration. This effect allows a greater fraction of the injected electrons to recombine with the oxidized dye, $N3^+$, or with electron-accepting impurities in solution. As a consequence, the possible gain in V_{oc} by using redox couples with more positive equilibrium potentials is not realized. Finally, the performance of $(SeCN)_2/SeCN^-$ is somewhat encouraging.

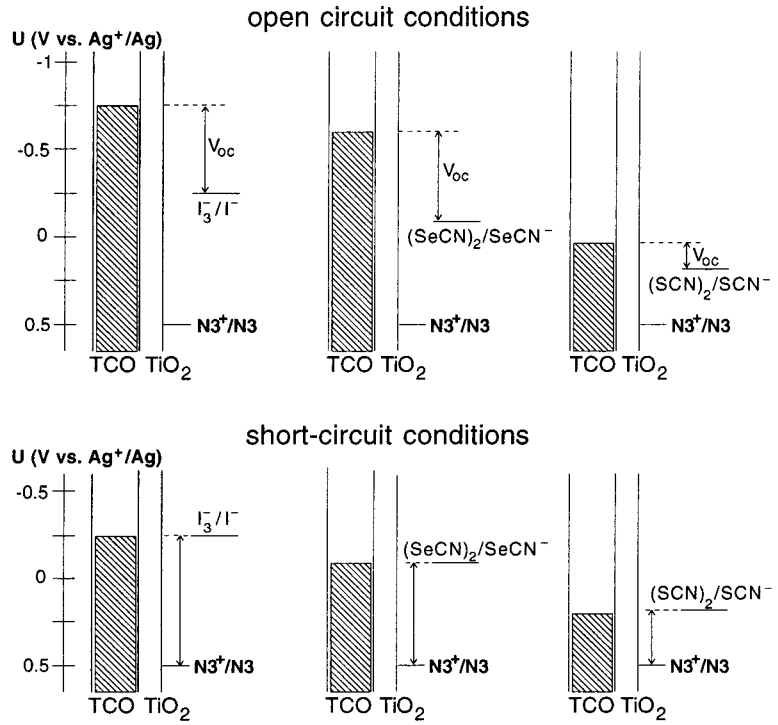

Figure 8. Energy band diagrams for the open circuit and short circuit conditions for the dye-sensitized TiO_2 photoelectrochemical cells with 0.25 M $LiClO_4$ in acetonitrile solutions with the I_3^-/I^-, $(SeCN)_2/SeCN^-$, and $(SCN)_2/SCN^-$ redox couples, respectively. The positions of the Fermi energies of the TCO/dye-sensitized TiO_2 working and TCO/Pt counter electrodes were determined from the results shown in Figure 7. It is assumed that the energy levels of the dye do not shift upon changing the redox couple. The arrows shown for the short circuit diagrams indicate the thermodynamic driving force for the regeneration of the dye by the electron donor in the solution.

To our knowledge, the only redox couple that has previously been reported to yield high photocurrents with this sensitizer is I_3^-/I^-. For other sensitizers, Br_2/Br^- and quinone/hydroquinone have also been successfully utilized.[28] The ~20% IPCE and V_{oc} comparable to in iodide/tri-iodide for *cis*-$Ru(dcb)_2(NCS)_2/TiO_2$ suggests that alternative sensitizers with more positive $U°(D^+/D°)$ may yield more efficient energy conversion with this alternative redox couple.

Conclusions

We have evaluated pseudohalogen redox couples in order to determine the effect of the equilibrium potential of the redox couple on the energetics and kinetics of dye-sensitized TiO_2 photoelectrochemical cells. The results showed that selecting a redox couple with a more positive equilibrium potential does not necessarily translate into an increase of the open circuit potential. This is explained by the observation that the potentials of both the TCO/dye-sensitized TiO_2 electrode and the TCO/Pt electrode shift with the equilibrium potential of the redox couple, hence, the simplified picture shown in Figure 1 is not valid. Upon shifting the redox equilibrium potential more positive, the incident photon-to-current conversion efficiency was found to decrease by a factor of 4 for $(SeCN)_2/SeCN^-$ and a factor of 20 for $(SCN)_2/SCN^-$ compared with I_3^-/I^-. Transient absorbance studies demonstrated that the lower efficiencies are related to a slower dye regeneration rate when SCN^- or $SeCN^-$ are used in place of I^-. As a consequence, a greater fraction of the injected electrons is allowed to recombine with the oxidized dye, $N3^+$, or with electron-accepting impurities in solution.

Acknowledgment. The authors gratefully acknowledge support from the Department of Energy under contract DE-FG02-98ER82567 and EIC Laboratories. G.J.M. and B.V.B. gratefully acknowledge support from the National Science Foundation, CHE-0078938.

Supporting Information Available. A typical preparation procedure for the N3 dye. This material is available free of charge via the Internet at http://pubs.acs.org.

References and Notes

(1) O'Regan, B.; Grätzel, M. *Nature* **1991,** ***353,*** **737.**

(2) For recent reviews see: (a) Qu, P.; Meyer, G. J. Dye Sensitized Electrodes in *Electron Transfer in Chemistry*; Balzani, V., Ed.; 2000, Vol. IV, Chapter 2, Part 2, pp 355−411. (b) Hagfeldt, A.; Grätzel, M. *Acc. Chem. Res.* **2000**, 33, 269−277. (c) Hagfeldt, A.; Grätzel, M. *Chem. Rev.* **1995**, *95*, 49−73.

(3) Nazeeruddin, M. K.; Kay, A.; Rodicio, I.; Humphry-Baker, R.; Müller, E.; Liska, P.; Vlachopoulos, N.; Grätzel, M. *J. Am. Chem. Soc.* **1993**, *115*, 6382−6390.

(4) Huang, S. Y.; Schlichthörl, G.; Nozik, A. J.; Grätzel, M.; Frank, A. J. *J. Phys. Chem. B* **1997**, *101*, 2576−2582.

(5) Argazzi, R.; Bignozzi, C. A.; Heimer, T. A.; Castellano, F. N.; Meyer, G. J. *J. Phys. Chem. B* **1997**, *101*, 2591−2597.

(6) Bonhote, P.; Grätzel, M.; Jirousek, M.; Liska, P.; Pappas, N.; Vlachopoulos, N.; von Planta, C.; Walder, L. *Tenth International Conference on Photochemical Conversion and Storage of Solar Energy*, 1994, Abstract C2.

(7) Pelet, S.; Moser, J. E.; Grätzel, M. *J. Phys. Chem. B* **2000**, *104*, 1791−1795.

(8) (a) Nasr, C.; Hotchandani, S.; Kamat, P. V. *J. Phys. Chem. B* **1998**, *102*, 4944−4951. (b) Thompson, D. W.; Kelly, C. A.; Farzad, F.; Meyer, G. J. *Langmuir* **1999**, *15*, 650−653.

(9) Papageorgiou, N.; Liska, P.; Kay, A.; Grätzel, M. *J. Electrochem. Soc.* **1999**, *146*, 898−907.

(10) (a) Kelly, C. A.; Thompson, D. W.; Farzad, F.; Stipkala, J. M.; Meyer, G. J. *Langmuir* **1999**, *15*, 7047−7054. (b) Yates, D. E.; Healy, T. W. *J. C. S. Faraday Trans. 1* **1980**, *76*, 9−18. (c) Berubé, Y. G.; DeBruyn, P. L. *J. Colloid Interface Sci.* **1968**, *28*, 92−105.

(11) (a) Wang, C. M.; Mallouk, T. E. *J. Phys. Chem.* **1990**, *94*, 423−428. (b) Wang, C. M.; Mallouk, T. E. *J. Phys. Chem.* **1990**, *94*, 4276−4280.

(12) Fitzmaurice, D.; Frei, H. *Langmuir* **1991**, *7*, 1129−1137.

(13) (a) Sodergren, S.; Hagfeldt, A.; Olsson, J.; Lindquist, S. E. *J. Phys. Chem.* **1994**, *98*, 5552−5556. (b) Cao, F.; Oskam, G.; Searson, P. C.; Meyer, G. J. *J. Phys. Chem.* **1996**, *100*, 17021−17027. (c) De Jongh, P. E.; Vanmaekelbergh, D. *Phys. Rev. Lett.* **1996**, *77*, 3427−3430. (d) Dloczik, L.; Ileperuma, O.; Lauermann, I.; Peter, L. M.; Ponomarev, E. A.; Redmond,

G.; Shaw, N. J.; Uhlendorf, I. *J. Phys. Chem. B* **1997**, *101*, 10281−10289. (e) Nelson, J. *Phys. Rev. B* **1999**, *59*, 15374−15380. (f) Van de Lagemaat, J.; Park, N. G.; Frank, A. J. *J. Phys. Chem. B* **2000**, *104*, 2044−2052.

(14) (a) See Supporting Information. (b) Nazeeruddin, M. K.; Kay, A.; Rodicio, I.; Humphry-Baker, R.; Müller, E.; Liska, P.; Vlachopoulos, N.; Grätzel, M. *J. Am. Chem. Soc.* **1993**, *115*, 6382−6390. (c) Sullivan, B. P.; Salmon, D. J.; Meyer, T. J. *Inorg. Chem.* **1978**, *17*, 3334−3341.

(15) (a) Wood, J. L. *Org. React.* **1946**, *3*, 240−266. (b) Bacon, R. G. R.; Irwin, R. S. *J. Chem. Soc.* **1958**, *Pt. 1*, 778−784.

(16) Bowmaker, G. A.; Kilmartin, P. A.; Wright, G. A. *J. Solid State Electrochem.* **1999**, *3*, 163−171.

(17) Bard, A. J.; Faulkner, L. R. *Electrochemical Methods: Fundamentals and Applications;* Wiley: New York, 1980. (b) Pavlishchuk, V. V.; Addison, A. W. *Inorg. Chim. Acta* **2000**, *298*, 97−102.

(18) O'Regan, B.; Moser, J.; Anderson, M.; Grätzel, M. *J. Phys. Chem.* **1990**, *94*, 8720−8725.

(19) Kelly, C. A.; Farzad, F.; Thompson, D. W.; Meyer, G. J. *Langmuir* **1999**, *15*, 731−737.

(20) Southampton Electrochemistry Group, *Instrumental Methods in Electrochemistry*; Ellis Horwood: New York, 1990.

(21) Macagno, V. A.; Giordano, M. C.; Arvía, A. J.; Calandra, A. J. *Electrochim. Acta* **1969**, *14*, 335−357.

(22) Cauquis, G.; Pierre, G. *C. R. Acad. Sci. Paris* **1968**, *266C*, 883−886.

(23) Pereiro, R.; Arvía, A. J.; Calandra, A. J. *Electrochim. Acta* **1972**, *17*, 1723.

(24) Cauquis, G.; Pierre, G. *C. R. Acad. Sci. Paris* **1969**, *269C*, 740−743.

(25) Bard, A. J.; Parsons, R.; Jordan, J., Eds. *Standard Potentials in Aqueous Solutions*; Marcel Dekker: New York, 1985.

(26) Elliot, A. J. *Can. J. Chem.* **1992**, *70*, 1658−1661.

(27) Enright, B.; Redmond, G.; Fitzmaurice, D. *J. Phys. Chem.* **1994**, *98*, 6195.

(28) Desilvestro, J.; Grätzel, M.; Kavan, L.; Moser, J.; Augustynski, J. *J. Am. Chem. Soc.* **1985**, *107*, 2988−2990.